ELSEVIER

Chemical Engineering Journal 141 (2008) 35–41

Chemical Engineering Journal

www.elsevier.com/locate/cej

Optimization of the AZO dyes decoloration process through neural networks: Determination of the H_2O_2 addition critical point

Oswaldo Luiz Cobra Guimarães *, Darcy Nunes Villela Filho, Adriano Francisco Siqueira, Helcio José Izário Filho, Messias Borges Silva

School of Engineering of Lorena, University of São Paulo, CEP 12602-810, SP, Brazil

Received 20 March 2007; received in revised form 23 July 2007; accepted 10 October 2007

Abstract

The concentration of hydrogen peroxide is an important parameter in the azo dyes decoloration process through the utilization of advanced oxidizing processes, particularly by oxidizing via UV/H_2O_2. It is pointed out that, from a specific concentration, the hydrogen peroxide works as a hydroxyl radical self-consumer and thus a decrease of the system's oxidizing power happens. The determination of the process critical point (maximum amount of hydrogen peroxide to be added) was performed through a "thorough mapping" or discretization of the target region, founded on the maximization of an objective function objective (constant of reaction kinetics of pseudo-first order). The discretization of the operational region occurred through a feedforward backpropagation neural model. The neural model obtained presented remarkable coefficient of correlation between real and predicted values for the absorbance variable, above 0.98. In the present work, the neural model had, as phenomenological basis the Acid Brown 75 dye decoloration process. The hydrogen peroxide addition critical point, represented by a value of mass relation (F) between the hydrogen peroxide mass and the dye mass, was established in the interval $50 < F < 60$.

Keywords: H_2O_2/UV; Decoloration; Neural networks; Optimization

1. Introduction

In the industry, optimization processes involve the minimization or maximization of an objective function objective, described in technical terms, economical terms or in both aspects. In general, the decision variables are subject to restrictions, being it of security, maximum and minimum operational limits or linked to the process modeling equations [1].

Regarding the photooxidizing processes based on the UV/H_2O_2 action, it is pointed out that one of the economical and process performance issues is related to the amount of hydrogen peroxide to be added in the process. However, a number of process variables, such as pH and temperature of the reaction media, concentration of the compounds to be degraded, time of exposition to ultraviolet light and presence of inorganic salts [2] are factors that, isolatedly, influence the process performance. In this case, the process becomes a system with multiple variables and, in this sense, neural networks appear as a modeling methodology that can be applied to multidimensional systems.

In recent years, neural networks have been applied in various areas in the chemical engineering and, concerning the advanced oxidizing processes, it can be quoted the work of Pareek et al. [3] in which it was studied the photodegrading of Spent Bayer liquor, with the use of a feedforward-type neural network. Pearson correlation coefficients above 0.99 were obtained in this work.

Slokar et al. [4] utilized Kohonen type neural networks for modeling the Reactive Red 120 dye decoloration process, as a function of the use of H_2O_2/UV.

Salari et al. [5] also applied the neural modeling technique for treating waters contaminated with *methyl tert-butyl ether* (MTBE) by the combined use of hydrogen peroxide and ultraviolet radiation. In this work, the authors utilized a feedforward-type network to predict the MTBE concentration after photooxidizing treatment, obtaining Pearson correlation coefficients equal to 0.998.

* Corresponding author. Tel.: +55 12 31525996.
E-mail addresses: oswaldocobra@debas.faenquil.br (O.L.C. Guimarães), darcy@debas.faenquil.br (D.N.V. Filho), adriano@debas.faenquil.br (A.F. Siqueira), helcio@dequi.faenquil.br (H.J.I. Filho), messias@dequi.faenquil.br (M.B. Silva).

1385-8947/$ – see front matter © 2007 Elsevier B.V. All rights reserved.
doi:10.1016/j.cej.2007.10.017

Nomenclature

[dye]	dye concentration
GD = $\frac{\text{absorbance}_o - \text{absorbance}_i}{\text{absorbance}_o}$	decoloration degree
A	predicted values of absorbance
Absorbance_i	absorbance after decoloration
Absorbance_o	initial absorbance
ABr	Acid Brown 75
c_1	constant of integration
Co	number of neurons of the hidden layer
CP	coefficient of correlation of Pearson
f	transference function
F	mass relation between the hydrogen peroxide mass and the dye mass
k	reaction constant
m_0	initial hydrogen peroxide mass
m_1	dye mass
m_{dye}	dye mass
MSE	mean square error
N	number of sample points
ptr	set of training (input)
R	Pearson correlation coefficients
T	real values of absorbance
T_i	temperature of each experiment
TO	photooxidizing process operation time
TOC	total organic carbon
$V_{H_2O_2}$	hydrogen peroxide volume
w_i	the pondering weights of these signals or information
x_i	values of the inlet signals
X	vector das Entradas ao Neurônio
y_t	the values predicted by the neural network
Y_t	real values

Greek letters

η	Constante de momentum
λ	maximum wavelengths

Guimarães and Silva [6] utilized a feedforward backpropagation neural network model for modeling the decoloration process (via H_2O_2/UV) of an azo dye group, where it was inserted structural characteristics of dyes such as the number azo bonds and sulphonate groups and process operational characteristics (temperature of the reaction system, pH, time of operation of the reactor, concentration of dyes and hydrogen peroxide). The model was classified as hybrid in relation to the nature of the inlet variables (operational and structural) and Pearson correlation coefficients of 0.96 were obtained.

Durán et al. [7] studied the degradation of the dye Reactive Blue 4 through the photo-Fenton process, with adjustment of the experimental data via the neural models. The mathematical model reproduced the experimental data (with average response values measured by the constants of reaction for the discoloration and mineralization processes) at an interval of reliance from 82 to 86%.

The present work aimed the determination of an optimum mass relation between the initial amount of hydrogen peroxide and the amount of dye involved in the decoloration process. For the analysis of this relation, was chosen the corante Acid Brown 75, manufactured for industry BASF, widely used in the industries textile and of leathers. It is observed that works related to the degradation or discoloration of this corante had not been found in the bibliography.

2. UV/H_2O_2 process

It is widely accepted that the first step in the UV/H_2O_2 process is the attack of the photon against the hydrogen peroxide molecule and the subsequent formation of hydroxyl radical $^\bullet$OH [8]:

$$H_2O_2 + h\upsilon \rightarrow 2^\bullet OH \quad (1)$$

High concentrations of H_2O_2 do not necessarily favor the kinetics of the reaction, for after the reaction starts, the steps of propagation can be prevented by the excess of hydrogen peroxide. This excess can act as a hydroxyl radical self-consumer [9], according to the reaction given by Eq. (2).

$$H_2O_2 + {}^\bullet OH \rightarrow H_2O + HO_2{}^\bullet \quad (2)$$

Besides water, reaction (2) produces the hydroperoxyl radical, less reactive than the hydroxyl radical.

Thus, hydrogen peroxide in excess may react with the hydroxyl radical and compete with the attack of this radical to the dye in the solution during the photolysis [10].

Considering that the recombination reactions (Eqs. (3)–(6) may occur, there is the possibility of hydroxyl radical consumption, decreasing the probability of the organic compounds oxidation. Thus, a competition for the ultraviolet light starts.

$$H_2O_2 + {}^\bullet O_2H \rightarrow {}^\bullet OH + H_2O + O_2 \quad (3)$$

$$^\bullet OH + {}^\bullet OH \rightarrow H_2O_2 \quad (4)$$

$$^\bullet O_2H + {}^\bullet O_2H \rightarrow H_2O_2 + O_2 \quad (5)$$

$$^\bullet OH + {}^\bullet O_2H \rightarrow H_2O + O_2 \quad (6)$$

The kinetics of the reaction is favored up to the H_2O_2 addition critical point. The critical point is related to various factors such as the amount of hydrogen peroxide added, reaction media pH, UV radiation wavelength, dye concentration and structural characteristics, besides other specific factors like the presence of inorganic salts, which affect the reaction performance of the hydroxyl radical.

3. Materials and methods

Hydrogen peroxide 30% (w/w) was used in all photooxidizing procedures and solutions of NaOH and H_2SO_4 at 0.5 eq/L were used for the adjustment of the reaction mean initial pH. The pH was kept constant during the reaction. Distilled water was utilized in the composition of all processes.

The Acid Brown 75 decoloration was evaluated as a function of the absorbance measured every 5 min, via Femto 600

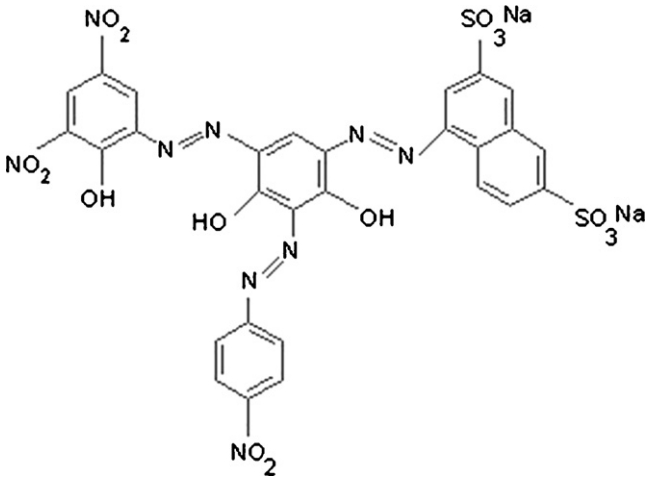

Fig. 1. Acid Brown 75 molecular structure.

spectrophotometer, at the maximum absorbance wavelength (430 nm), optimized from the dye absorbance spectrum in aqueous solution.

The mineralization extents were determined on the basis of total organic carbon content measurements (TOC), performed by using total organic carbon analyzer; TOC-ASI 5000A, Shimadzu.

Fig. 1 presents the structure of the dye studied.

The photooxidizing process was performed in a Germetec GPJ 463-1 plug-flow reactor, with low pressure radiation source of 21 W, and at the end of each experiment, the system, for washing purposes, was filled with slight acid solution and recirculated.

Fig. 2 presents the laboratorial scheme utilized in the photooxidizing process.

After the discharge of the solutions and recirculation with distilled water, the system was dismounted and the reactor filled with nitric acid solution 10% (v/v) for cleaning. The temperature in each experiment was kept constant through Optherm DC1 thermostatic bath, in $T \pm 2\,^{\circ}C$, where T is the temperature of each experiment, within a range of 22–45 °C.

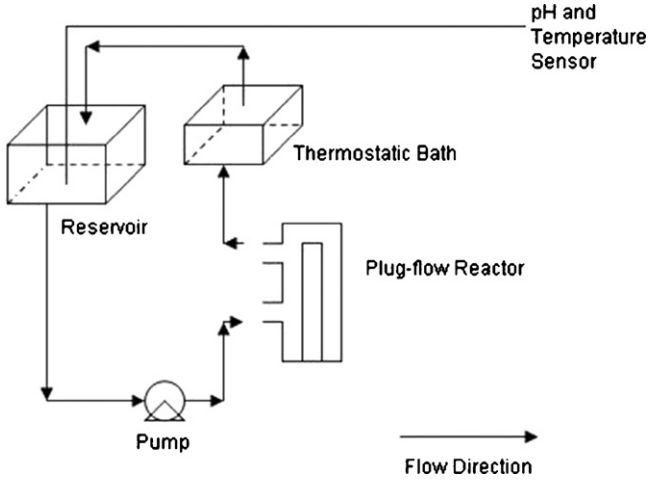

Fig. 2. Laboratorial scheme.

Table 1
Levels of the operational variables

	pH	TO (min)	[dye] mg/L	$V_{H_2O_2}$ (mL)	T (°C)
Minimum (−1)	2	15	30	2	22
Maximum (+1)	11	150	100	22	45

Table 1 defines the levels of the operational variables utilized in the experiments.

4. Artificial neural networks

Neural networks may be defined as "a set of mathematical methods and computational algorithms designed to simulate the information processing and the acquisition of knowledge on the human brain". The neural networks basic elements are the artificial neurons, synapses, neural weights, transference functions, neural networks architecture and neural networks training [11].

In an analogy to the biological neurons, the artificial neurons have a central processing structure (usually called net) and inlet (dendrites) and outlet (axon) ramifications.

Not going deeper on the physical–chemical processes involved in the transmission of information between the biological neurons, the signal enters the neurons through the dendrites, passes through the cellular body and is then transmitted to other neurons of the network by means of the axons. The transmission of the signal of a neuron to the dendrites of another neuron is called synapse, which is basically the function of modulating the signal exchanged between them. In the artificial neuron, this modulation of the signal, or signal intensity, is represented by a pondering factor called synaptic weight.

The value of the total signal that enters the neuron central body is called net and can be estimated through the multiplication of the signal that comes into the neuron times the synapse weight of this signal. As the neurons have a large number of dendrites and, thus, being able to establish various synapses with other neurons, the value of the total signal that comes to the neuron can be mathematically represented by Eq. (7):

$$\text{Net} = \sum_{i=1}^{n} w_i x_i \tag{7}$$

The neuron outlet, thus, is obtained as a function of the inlet signal, that is, it can be considered that outlet = f(net), where f is the transference function.

The transference function is necessary for the transformation of the sum of the neurons inlet signals pondered weight in order to determine the outlet signal value or intensity, being that one of the most used functions is the sigmoidal function:

$$f(\text{net}) = \frac{1}{1 + e^{-\text{net}}} \tag{8}$$

The function of linear activation for the outlet layer is adequate for continuous phenomena, as for instance the oxygen biochemical demand or absorbance decrease in decoloration processes. The sigmoidal-type transference functions are necessary to introduce non-linearity in the network.

In order to determine the synaptic weight values a training process is performed. The neural network training is a function of the neural weights update, through a process called learning through error corrections, where the values simulated by the neural network are compared to the desired values. This way, the objective is to determine the set of synaptic weights that minimize an error function, like the mean square error (MSE) equation defined by Eq. (9) [12]:

$$\varepsilon = \mathrm{MSE} = \sum_{i=1}^{N} \frac{(Y_t - \hat{y}_t)^2}{N} \tag{9}$$

The training algorithm named backpropagation refers to the way the weights are adjusted, and this algorithm is also known as Generalized Delta Rule.

In the Generalized Delta Rule, in order to minimize the mean square error, the derivatives defined by Eq. (10) are estimated.

$$\vec{\nabla}_j^k = \frac{\partial \varepsilon}{\partial W_j^{(k)}} \tag{10}$$

The backpropagation algorithm utilizes the information of these derivatives (gradient) for the moving on change of the weights according to Eq. (11):

$$W_j^{(k)}(n+1) = W_j^{(k)}(n) + \mu(-\vec{\nabla} W_j^{(k)}(n)) \tag{11}$$

In Eq. (11), $\mu > 0$ is the network learning rate, which controls the degree according to which the gradient affects the weights change and n means the current iteration [13].

It is possible to improve the speed of convergence of the artificial neural network trained by the backpropagation algorithm through the utilization of this momentum. The purpose of this method is to add, when estimating the value of change of the synaptic weight, a fraction proportional to the prior alteration. So, the introduction of this term in the equation of adaption of the weights tends to improve the stability of the learning process, favoring changes in the same direction and impeding local minimums. The addition of the term momentum to accelerate the learning process and avoid local minimums is frequently utilized in the neural modeling, suppressing the oscillation of weights in valleys and ravines.

In such a way, Eq. (11) can be substituted by Eqs. (12) and (13):

$$\Delta W_j^{(k)}(n) = 2\mu(1-\eta)\delta_j^{(k)} X_j^{(k)}(n) + \eta\, \Delta W_j^{(k)}(n-1) \tag{12}$$

$$W_j^{(k)}(n+1) = W_j^{(k)}(n) + \Delta W_j^{(k)}(n) \tag{13}$$

In Eqs. (12) and (13) $0 \leq \eta \leq 1$ is the momentum constant.

The neural network adopted in the present work comprises three layers: inlet, hidden and outlet. Some theorems have already been found out about the networks characteristics [13]:

(a) if a function consists of a finite collection of points, then a three layer network is able to learn it;
(b) in case this function is continuous and defined in a compact dominium, a three layer network is able to learn it, since there are sufficient processing elements in the hidden layer.

5. Complete mapping by neural networks

An experimental design (2^5) was implemented making up 32 experiments for the dye. The 5 min interval data collection provided the formation of a neural network input matrix of 528 lines (samples) by 5 columns (process input variables) with the addition of some random experiments. The addition of these randon points was made in central and intermediate points to the extremes of the variables. The output factor of a neural model was constituted of 528 absorbance values in the range of [0,2].

The neural model input and output values were normalized in such a way that the average value would be zero and the standard deviation equal to 1.

The sample set deriving from the experiments was divided in training (50%), validation (25%) and test (25%).

The feedforward neural model has been implemented in MatLab software, with the following characteristics:

- net.trainParam.goal = 1E−8; aimed training final error.
- net.trainParam.lr = 0.1; learning rate.
- net.trainParam.show = 25; screen actualization (epochs).
- net.train.Param.mc = 0.87; momentum rate.
- net.trainParam.lr _inc = 1.15; l.r. increment rate.
- net.trainParam.lr_dec = 0.75; Ir decrement rate.
- net.trainParam.max_max_perf_inc = 1.04; error maximum increment.
- net.performFcn = 'mse'.
- net = newff(minmax(ptr),[co], {'tansig' 'purelin'}, 'traingdm').

Co represents the hidden layer number of neurons and ptr stands for the network inlet values training set (dye concentration, pH, time of operation, temperature and H_2O_2 volume). The outlet variable was the solution absorbance.

A scheme for implementing the optimization process by means of "complete" mapping of values simulated by the neural model can be visualized in Fig. 3.

After the training and validation phases of the neural model obtained, the mapping of the operational conditions was performed. This phase comprised the discretization of all possible process inlet variables. The multifunctional points discretized and simulated by the neural model generated discretized absorbance values. The discretization period was equal to 0.01 when simulating the neural model obtained.

Once simulated the discretization process to obtain the absorbance values, the linear regression (time of operation versus absorbance) was performed (least square method) for the adjustment of the constant of reaction (k) in a pseudo-first order model, mapping the values of this constant through the discretization of the inlet variables, up to the obtainment of its maximum value of this constant.

The following restrictions were imposed during the training phase and complete mapping or discretization.

$$22\,^{\circ}\mathrm{C} \leq T_{\mathrm{i}} \leq 45\,^{\circ}\mathrm{C} \tag{14}$$

$$30\,\mathrm{mg/L} \leq [\mathrm{dye}] \leq 100\,\mathrm{mg/L} \tag{15}$$

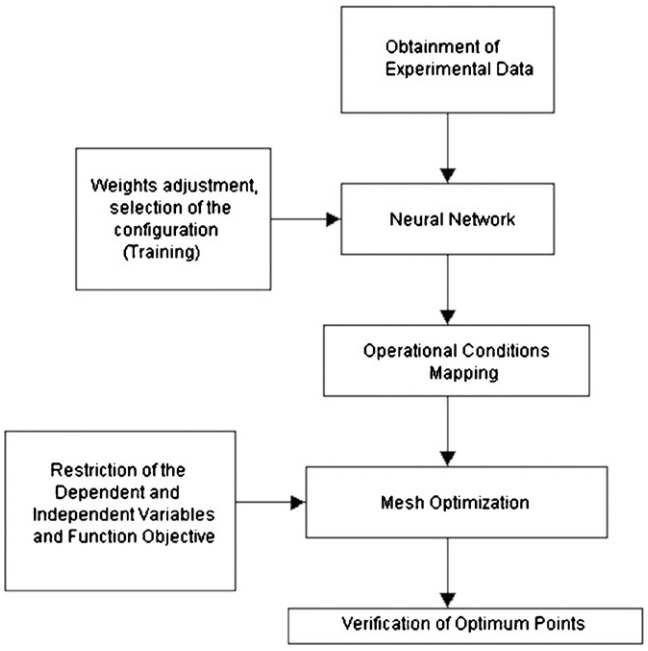

Fig. 3. Implementation of the optimization process.

$$\mathrm{GD} = 0.90 \tag{16}$$

$$2 \leq \mathrm{pH} \leq 11 \tag{17}$$

$$15 < \mathrm{TO} \leq 150 \tag{18}$$

$$2\,\mathrm{ml} \leq V_{H_2O_2} \leq 22\,\mathrm{ml} \tag{19}$$

Thus, the objective was to determine the process inlet variables values that provided the maximum value of the reaction constant, with the restriction of being reached a decoloration degree imposed as a maximum of 90% for this study.

The photooxidation is supposed to be a reaction of pseudo-first order and the kinetics of color degrading can be expressed by:

$$\frac{dC_{dye}}{dt} = -kC_{dye} \tag{20}$$

The integration of this expression produces:

$$\ln(C_{dye}) = -kt + c_1 \tag{21}$$

From this expression, by linear regression, the values of the constants of reaction kinetics were determined. These values made the composition of the objective function to be mapped in a discretized form by the neural model.

Table 2
Coefficients of correlation

Neurons hidden layer	R (training)	R (validation)	R (test)
8	0.965	0.954	0.923
12	0.976	0.971	0.963
15	0.982	0.980	0.979
16	0.987	0.981	0.984
20	0.951	0.934	0.921

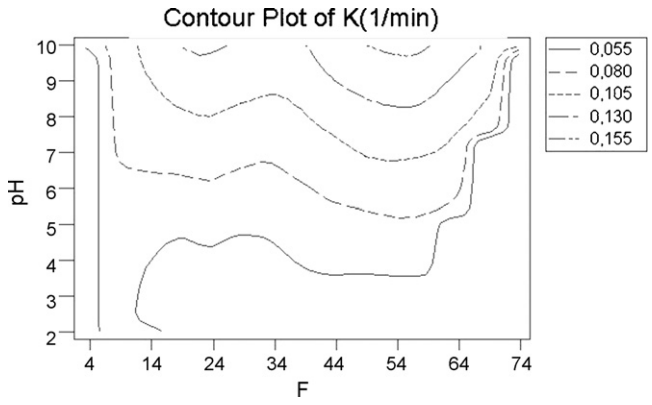

Fig. 4. Contour surface, ABr 75, $T_i = 45\,^{\circ}\mathrm{C}$, $15 < \mathrm{TO} < 150$.

Table 2 presents the results of the adjustments for the training (50%), validation (25%) and test (25%) sets. The percentages refer to the experimental data total set.

The values of the Pearson correlation coefficients above 0.98 for value predicted for absorbance and absorbance real value indicate a good adjustment and prediction capacity for the neural model. The neural model obtained (16 neurons in the hidden layer) mapped a multidimensional space of the form absorbance = ([dye], pH, T, TO, $V_{H_2O_2}$).

In order to avoid overtraining problems, the training was interrupted when the error corresponding to the validation set became higher than the error corresponding to the training set and, according to this criteria, a number of epochs equal to 49 was obtained.

The graphic verification of the H_2O_2 addition critical behavior was performed through surface graphs. The k reaction constant maximum value was reached experimentally for values of F in the range of 50–60, according to Eq. (22):

$$F = \frac{m_0}{m_1} \tag{22}$$

In Eq. (22), m_0 represents the initial hydrogen peroxide mass and m_1 stands for the dye mass.

The Fig. 4 exemplifies the contour surface graph obtained for experimental values.

Table 3 shows some results of the pseudo-first order adjustment, where the best performances of the process around a mass relation close to $F = 50.449$ is verified.

Table 3
Constant of pseudo-first order

F	K (min^{-1})	R
3.2450	0.0625	0.9989
9.9990	0.0971	0.9864
16.6650	0.1253	0.9985
26.7170	0.1296	0.9966
33.0330	0.1326	0.9912
50.4490	0.1564	0.9958
53.2216	0.1481	0.9982
56.3206	0.1386	0.9956
73.6900	0.1112	0.9975
100.0900	0.1097	0.9965

Table 4
Some results of the complete mapping

pH	m_{dye}	F_{real}	$F_{predicted}$
9.8	100	$50 < F < 60$	55.55
10.0	120	$50 < F < 60$	51.33
10.5	130	$50 < F < 60$	52.22
10.1	140	$50 < F < 60$	58.00
9.9	150	$50 < F < 60$	50.00
9.6	200	$50 < F < 60$	57.89
9.4	250	$50 < F < 60$	58.90
10.0	300	$50 < F < 60$	53.76

In Table 4, some results from contour surfaces graphs are presented, for different operational conditions.

Table 5 presents some results obtained during the processo f discoloration of the Abr 75, where the efficiency of the process in function of the utilization of UV/H_2O_2 is verified. Table 5 also presents percentage of reduction of the TOC, indicating the degree of mineralization of the dye proving that the method may be considered ecologically applicable.

The effects of the variation of the levels of the inlet variables can be observed in Fig. 5, where it is noticed that the higher degree of discoloration obtained occurred in the high pH, temperature and UV reactor time of operation levels. Concerning

Table 5
Degree of discoloration and mineralization

pH	Temperature	$V(H_2O_2)$	[Dye]	TO	GD	%TOC
1	1	1	1	1	100	96.00
−1	1	−1	−1	−1	95.02	90.27
−1	−1	1	−1	1	100.00	96.89
1	−1	1	1	1	98.82	93.89
−1	−1	−1	−1	1	100.00	94.21
−1	1	1	1	−1	85.70	75.54
−1	−1	−1	1	−1	90.20	80.29
1	−1	1	−1	−1	93.97	82.56
1	1	1	1	−1	99.74	89.00
−1	1	−1	1	1	92.13	81.09
−1	1	−1	1	−1	86.49	75.66
−1	1	1	−1	1	93.95	83.62
1	−1	−1	1	−1	77.26	69.02
1	1	1	−1	1	100.00	92.01
1	−1	1	1	−1	88.19	80.98
1	−1	1	−1	1	100.00	91.98
−1	−1	−1	1	1	93.57	86.09
1	−1	−1	1	1	98.67	90.77
−1	1	1	−1	−1	87.97	85.33
−1	1	1	1	1	89.54	86.86
1	1	−1	−1	−1	99.76	98.78
1	−1	−1	−1	−1	98.56	94.56
1	−1	−1	−1	1	98.35	89.90
1	1	1	−1	−1	100.00	95.62
−1	−1	1	−1	−1	77.22	67.06
−1	−1	1	1	1	98.27	89.34
1	1	−1	−1	1	100.00	97.00
−1	−1	−1	−1	−1	82.50	81.23
−1	−1	1	1	−1	85.80	74.78
1	1	−1	1	1	100.00	98.12
1	1	−1	1	−1	99.62	92.34
−1	1	−1	−1	1	90.25	88.00

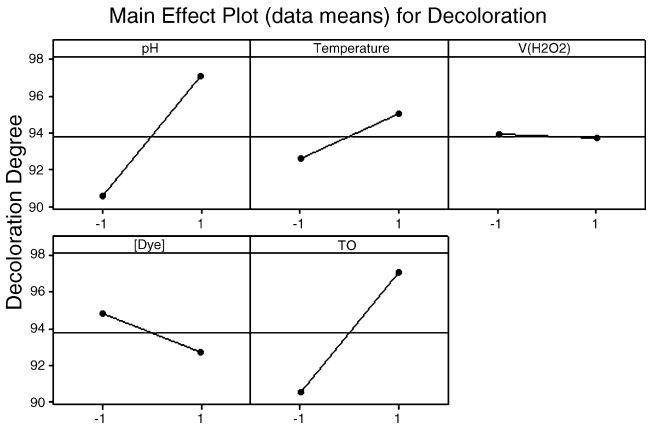

Fig. 5. Main effects—degree of discoloration.

the hydrogen peroxide, it is noticed that a small reaction yield decrease happened when the value changed from the smallest to the highest level and the same happened with the dye concentration. This result, in relation to the volume of hydrogen peroxide added, was an indication of a maximum hydrogen peroxide value to be added, from which the process of discoloration loses yield.

In case that it is not kept constant, it is important to point out that the pH tends to an acid or slightly acid means during the process of discoloration and that the pH variation is due to the increase of [H^+] concentration. The discoloration rate decreases as the production of hydroxone ion increases, what indicates that acid products can be resistant to the color degradation.

However, the characteristic of higher yield of the procsee of discoloration in alkaline pH is not prevalent for all dyes, for the work of Galindo and Kalt [14] can be cited, in which the process of discoloration was more effective in acid means. Neverthless, the authors report that for the dye Acid Orange 52 showed better performances of discoloration in neutral or slightly alkaline means.

Muruganandham and Swaminathan [15] report that the decrease of performance in alkaline means. The conjugated base of the hydrogen peroxide (HO_2^-) can react with the hydroxyl radical, consequently reducing the rate of discoloration, according to Eqs. (23) and (24):

$$H_2O_2 + HO_2^- \rightarrow H_2O + O_2 + {}^\bullet OH \quad (23)$$

$${}^\bullet OH + HO_2^- \rightarrow H_2O + O_2^- \quad (24)$$

Chu and Ma [16] noticed that for poliazo dyes, when the pH is low, the amount of radicals $^\bullet$OH are inadequate for the simultaneous attack to the −N=N− bonds of the dye molecule and, thus, the reaction of photodiscoloration for the poliazo dye tends to be incomplete in low pH. On the other hand, this effect is not observed, for the hydroxyl radicals are in higher amount. The authors also noticed that the π bond electrons are usually more diffuse and less steadily linked to the nitrogen atoms. Thus, they are particularly more susceptible to electrophilic agents like the hydroxyl radicals. However, at low pH, H^+ can interfere in the poliazo dyes conjugated system through the formation of positively charged central amines, which tend

to decrease the density of the azo groups and then describe the reactivity in relation to the hydroxyl radical, according to Eq. (25):

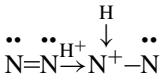

(25)

Theoretically, the rate of discoloration in alkaline pH can increase due to the neutralization of the H^+ ion generated in the photodiscoloration process. Shu et al. [10] enhance this result pointing out that the relationship of better performance for the initial pH condition depends on the type of dye to be degraded. In the study, for the Acid Orange 5, the authors report the best yield of the reaction for pH close to value 2.

Thus, each dye structural condition or conditions of compounds present together with the dyes can affect the behavior of the reaction in relation to the pH, and consequently the performance of the process of discoloration.

Some aspects must also be emphasized concerning the amount of H_2O_2 added. It is widely considered that the first step in the H_2O_2/UV process is the attack of the photon to the hydrogen peroxide and the formation of radicals [8], according to Eq. (26):

$$H_2O_2 + h\upsilon \rightarrow 2^{\bullet}OH \quad (26)$$

High peroxide concentrations do not necessarily favor the kinetics, for after the initial step the steps of propagation can be impeded by the excess of peroxide acting as an $^{\bullet}OH$ radicals self consumer [9], reaction given by Eq. (27):

$$H_2O_2 + {}^{\bullet}OH \rightarrow H_2O + HO_2{}^{\bullet}. \quad (27)$$

Thus, hydrogen peroxide in excess can react with the hydroxyl radical and compete with this radical attack to the dye in the solution by the time of photolysis [10,17], for the recombination reactions may occur consuming the hydroxyl radical and decreasing the probability of occurrence of the oxidation of organic compounds, So, a competition for the ultraviolet light starts: there is a critical point for the hydrogen peroxide concentration value. Up to this point, the kinetics of discoloration is favored by the increase of hydrogen peroxide concentration. This critical point is related to various factors such as the amount of hydrogen peroxide added, reaction mean pH, UV radiation emission wavelength, dye concentration and specification, besides each process other specific factors linked to the utilization of other dyes as, for instance, the addition of intermediates in the dyeing process, as, for example, the presence of sodium chlorides and sulphates.

6. Conclusions

The implementation of a neural model and the optimization through complete mapping of the dominium of the independent variables in a process of decoloration by UV/H_2O_2 is presented as a promising technique in the optimization of processes with multiple inlet variables.

The neural model reached good prediction capacity with Pearson correlation coefficients above 0.98 for the training, validation and test sets.

From this neural model, the discretization of all process variables could be performed, which made possible the search for the Acid Brown 75 dye decoloration process critical point through the use of UV/H_2O_2. The determination of the critical point, or maximum amount of hydrogen peroxide to be added as a function of the dye initial mass, was established in a $50 < F < 60$ interval, coinciding with the real values obtained in the experiments.

References

[1] C.A.O. Nascimento, R. Guardani, R. Giudici, Neural network based approach for optimization of industrial chemical process, Comput. Chem. Eng. 24 (2000) 2303–2314.
[2] M. Muthukumar, N. Selvakumar, Studies on the effect of inorganic salts on decolouration of acid dye effluents by ozonation, Dyes Pigments 62 (2004) 221–228.
[3] V.K. Pareek, M.P. Brungs, A.A. Adesina, R. Sharma, Artificial neural network modeling of a multiphase photodegradation system, J. Photochem. Photobiol. A: Chem. 149 (2002) 139–146.
[4] Y.M. Slokar, J. Zupan, A.M. Marechal, The use of artificial neural network (ANN) for modeling of the H_2O_2/UV decoloration process. Part I, Dyes Pigments 42 (1999) 123–135.
[5] D. Salari, N. Daneshvar, F. Aghazadeh, A.R. Khataee, Application of artificial neural networks for modeling of the treatment of wastewater contaminated with methyl *tert*-butyl ether (MTBE) by UV/H_2O_2 process, J. Hazard. Mater. B125 (2005) 205–210.
[6] O.L.C. Guimarães, M.B. Silva, Hybrid neural model for decoloration by H_2O_2/UV involving process variables and strucutural parameters characteristics to azo dyes, Chem. Eng. Process. 46 (January (1)) (2007) 45–51.
[7] A. Durán, J.M. Monteagudo, M. Mohedano, Neural networks simulation of photo-Fenton degradation of Reactive Blue 4, Appl. Catal. B: Env. 65 (2006) 127–134.
[8] A. Aleboyeh, H. Aleboyeh, Y. Moussa, Critical effect of hydrogen peroxide in photochemical oxidative decolorization of dyes: Acid Orange 8, Acid Blue 74 and Methyl Orange, Dyes Pigments 57 (2003) 67–75.
[9] A. Mohey, J.A. Libra, U. Wiesmann, Mechanism and kinetic model for the decolorization of the azo reactive black 5 by hydrogen peroxide and UV radiation, Chemosphere 52 (2003) 1069–1077.
[10] H.Y. Shu, M.C. Chang, H.J. Fan, Decolorization of azo dye acid black 1 by UV/H_2O_2 process and optimization of operating parameters, J. Hazard. Mater. B113 (2004) 201–208.
[11] E.O. Cerqueira, J.C. Andrade, R.J. Poppi, Redes Neurais e suas aplicações em Calibração Multivariada, Química Nova 24 (6) (2001) 864–873.
[12] M.M. Hamed, M.G. Khalafallah, E.A. Hassanien, Prediction of wastewater treatment plant performance using artificial neural networks, Env. Model. Software 19 (2004) 919–928.
[13] C. Loesch, T.S. Sari, Redes Neurais Artificiais, Fundamentos e Modelos, Editora da FURB, 1996.
[14] C. Galindo, A. Kalt, UV-H_2O_2 oxidation of monoazo dyes in aqueous media: a kinetic study, Dyes Pigments 40 (1998) 27–35.
[15] M. Muruganandham, M. Swaminathan, Photochemical oxidation of reactive azo dye with UV-H_2O_2 process, Dyes Pigments 62 (2004) 269–275.
[16] W. Chu, C.W. Ma, Reaction kinetics of UV-decolourization for dye materials, Chemosphere 37 (5) (1998) 961–974.
[17] A.M. Dein, J.A. Libra, U. Wiesmann, Mechanism and kinetic model for the decolorization of the azo dye reactive black 5 by hydrogen peroxide and UV radiation, Chemosphere 52 (2003) 1069–1077.